

Instabilities and routes to chaos in a homogeneously broadened one- and two-mode ring laser

W. Klische and C. O. Weiss

Physikalisch-Technische Bundesanstalt, D-3300 Braunschweig, West Germany

(Received 11 March 1985)

A bidirectionally emitting ring laser ($^{15}\text{NH}_3$ at $376\text{-}\mu\text{m}$ wavelength) exhibits self-pulsing and chaos. The routes to chaos are found to be either a one-frequency-period-doubling route to chaos, or a one-frequency-two-frequencies-phase-locking-period-doubling route to chaos—windows within the chaotic range; the same as reported for a two-roll Bénard convection cell experiment. In single-mode operation an instability is observed under conditions compatible with the Lorenz model.

In an attempt to observe instabilities and chaos of a homogeneously broadened laser we have chosen the rotational $aR(2,0) v_2=1$ transition of $^{15}\text{NH}_3$ at $376\text{-}\mu\text{m}$ wavelength optically pumped by the $10 R(42)$ CO_2 -laser line,¹ which coincides with the $^{15}\text{NH}_3$ vibrational $aR(2,0)$ transition.

This far-infrared laser has high lower-pump-level population and a high rotational-transition matrix element providing high laser gain. The vibrational matrix element is relatively small so that the ac-Stark effect,² being the only source of inhomogeneous broadening in an optically pumped gas laser, is small. Homogeneous linewidths in far ir (FIR) lasers, determined by pressure broadening, are of the order of 1 MHz so that the "bad cavity" prerequisite for instabilities to occur³ does not mean an excessively lossy resonator.

A ring resonator was chosen (Fig. 1), which avoids holes in the resonator mirrors, usually employed in the FIR for coupling purposes, so that the laser oscillates in pure TEM_{00} modes. Standing waves are avoided by the resonator ring geometry. The pump-laser beam is of approximately the same diameter as the FIR mode. As fast FIR detectors micrometer-size Schottky diodes are employed.

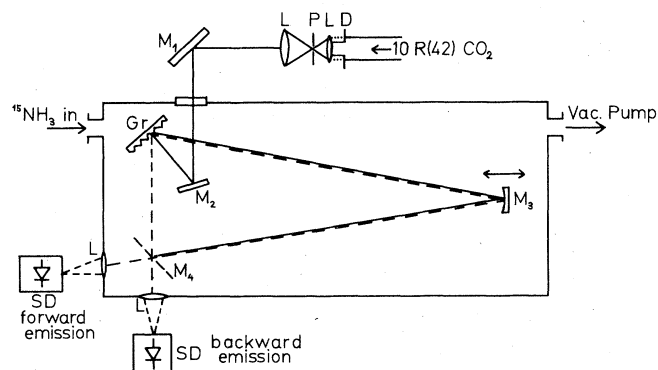


FIG. 1. FIR ring-laser setup. L: lenses; M_1, M_2, M_3 : gold mirrors; M_4 : gold wire mesh, $50\text{-}\mu\text{m}$ grid constant; Gr: $10\text{-}\mu\text{m}$ grating acting as specular reflector for FIR radiation; SD: Schottky barrier diodes acting as fast FIR detectors; P: pin hole; D: variable diameter diaphragm. Telescope LPL together with D serves as pump-intensity attenuator for a pump-beam geometry independent of pump intensity.

Table I gives constants of the NH_3 transition used that are relevant for comparisons of our observations with calculations.

Tuning the pump-laser frequency allows one, via the Doppler effect, to choose the velocity group of molecules providing the laser gain. Pumping substantially off the pump-absorption line center creates a situation where only the forward- or the backward-emitting laser mode interacts with the inverted molecules and the laser oscillates in a single traveling wave. Pumping close to or at pump line center allows both modes to interact with the inverted molecules.⁴ In this case, under cw conditions only one mode will oscillate due to competition. However, in the presence of instabilities both modes may emit. Thus, single-mode operation in the presence of instabilities requires off-center pumping and a gain linewidth (which in general is ac-Stark broadened in addition to homogeneous broadening), substantially narrower than the FIR Doppler width. This gives an upper limit of the operating pressure and the pump intensity.

I. TWO-MODE OBSERVATIONS

At a $^{15}\text{NH}_3$ pressure of 15 Pa and a maximum pump intensity of 1.5 W/cm^2 the routes to chaos given in Fig. 2 by the radio frequency (rf) power spectra of the laser output were observed when the pump intensity was progressively increased.

The laser first reaches the threshold for continuous single-mode emission and then the threshold for two-mode oscillation accompanied by a high-frequency self-pulsing. With higher pump power a second lower frequency appears as shown by the spectra consisting of all linear combinations of the two frequencies. The ratio of the two frequencies

TABLE I. Constants for the $376\text{-}\mu\text{m}$ $^{15}\text{NH}_3$ laser line.

Homogeneous linewidth HWHM	100 kHz Pa^{-1}
Doppler broadening HWHM	1.2 MHz
ac-Stark broadening HWHM	$26\text{ kHz}\sqrt{I}^a$
Population decay rate	100 kHz Pa^{-1}
Pump-transition dipole moment ^b	$4.0 \times 10^{-30} (1-M^2/9)^{1/2}\text{ C m}$
FIR-transition dipole moment ^b	$2.1 \times 10^{-29} (1-M^2/9)^{1/2}\text{ C m}$
Lower pump-level population	$1.3 \times 10^{18}\text{ Pa}^{-1}\text{ m}^{-3}$

^aIntensity I measured in mW/cm^2 . ^b M : magnetic quantum number.

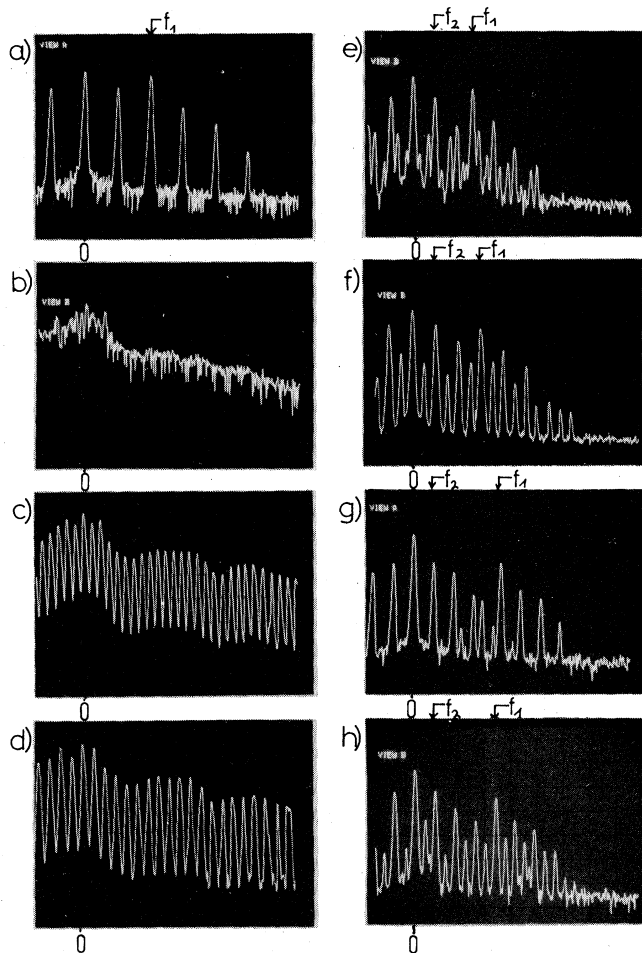


FIG. 2. Self-pulsing spectra of the two-mode ring laser. Vertical scale: 10 dB/division, horizontal scale: 500 kHz/division. (a) Period-doubled oscillation; (b) chaos; (c), (d) periodic windows above the threshold of chaotic emission; (e)–(h) two-frequency oscillation, phase locking, and period doubling; (e) f_2 slightly larger than $f_1/3$; (f) f_1 and f_2 lock at $f_2 = f_1/3$ and period double; (g) f_2 slightly smaller than $f_1/4$; (h) f_1 and f_2 lock at $f_2 = f_1/4$ and period double. Further period doublings following (f) and (h) lead to chaos. Also, phase locking at higher harmonics of f_2 was observed. Period doubling cascade between (a) and (b) as well as fundamental frequency preceding (a) left out for brevity. It was undecidable in the experiment whether (a) corresponds to a single-frequency oscillation or to an $f_2 = f_1/2$ locked state.

can be chosen by tuning of the pump frequency. Figure 2 shows different cases where the ratio is near 4, 3, and possibly 2. (It was not clear from the experiment whether 2 was a locked state with frequency ratio 2:1 or a state showing only one frequency and its first subharmonic.) Usually on increasing the pump power further, the two frequencies locked at the nearest harmonic of the lower frequency. Further increase of pump power then started the well-known parametric period-doubling cascade which leads to chaos. Sometimes locking was not observed but instead the two frequencies did persist up to the onset of chaos. Further increase of pump power in all cases allows one to observe several “windows” of regular oscillation in the chaotic range which also show period doubling.

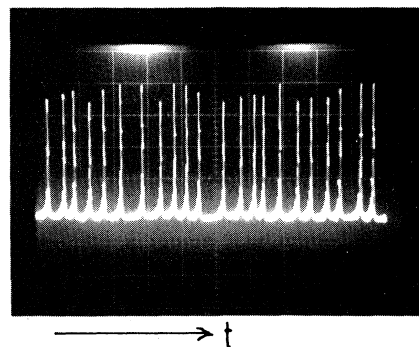


FIG. 3. Time picture of chaotic emission of two-mode NH_3 ring laser corresponding to the spectrum given in [Fig. 2(b)]: horizontal scale 50 μs /division.

Figure 3 shows a time picture of the laser emission in the chaotic range. It is quite apparent that the motion of the system is on a low-dimensional attractor. The emission, though characterized by a broadband noise spectrum, is relatively well ordered. The well-defined pulses from the region below chaos threshold persist, essentially only the time intervals between them varying at random. Under these conditions the ac-Stark broadening or splitting of the gain lines by the pump is smaller than the pressure broadening. Thus the laser can be characterized as homogeneously broadened, which should facilitate theoretical modeling. We note that this homogeneously broadened two-mode laser

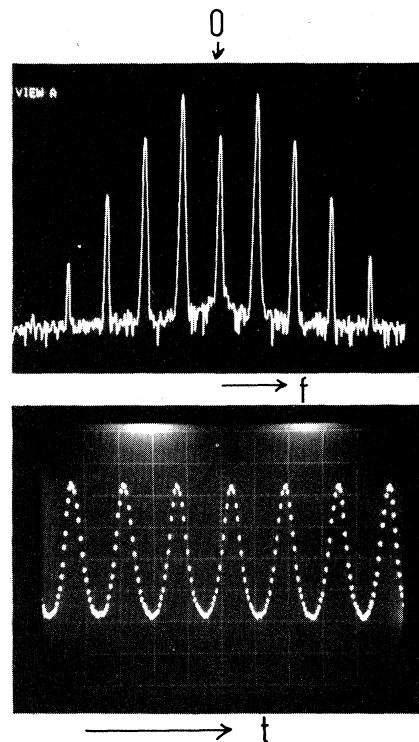


FIG. 4. Single-mode NH_3 ring-laser instability. NH_3 pressure 7 Pa, pump intensity 1 W/cm^2 . (a) rf spectrum, horizontal scale 1 MHz/division. (b) Time picture, horizontal scale 1 μs /division.

TABLE II. Characterization of the $^{15}\text{NH}_3$ laser at threshold of the single-mode instability for different pressures. The values for the ac-Stark broadening are an upper bound, calculated including M degeneracy and mixed broadening. They correspond to the intensity at the entrance of the resonator and will decrease along the resonator round trip due to absorption. The ac-Stark broadening integrated over one round trip will thus be smaller. ac-Stark broadening given allows for absorption of the pump radiation in the laser gas before the radiation enters the FIR resonator.

Pressure (Pa)	cw-laser pump threshold (mW/cm ²)	Instability pump threshold (mW/cm ²)	Homogeneous linewidth HWHM (kHz)	ac-Stark linewidth pump threshold	Instability pump threshold	cw-laser pump threshold
8	80	760	800	350		9.5
6	48	600	600	300		12.5
5	28	400	500	250		14.5
4	16	300	400	220		18.8

shows the same dynamics as reported for a (two-roll) Bénard convection cell.⁵ The dynamics of this system is different from the two-mode CO_2 -ring laser recently reported.⁶ The reason is that, other than with the CO_2 laser, the three relaxation times of the laser are of the same order of magnitude so that none of them can be adiabatically eliminated.

II. ONE-MODE OBSERVATIONS

The question arises whether this NH_3 laser can reach instabilities in single-mode emission under homogeneous broadening conditions and thus be suitable to test experimentally the predictions of the Lorenz model.³

Experiments were therefore carried out at lower gas pressures with the pump laser detuned from NH_3 -absorption line center. At a pump power of $\leq 1 \text{ W/cm}^2$ an oscillatory instability occurs for pressures below 8 Pa. The oscillation is slightly nonsinusoidal. A typical time picture and rf spectrum of the laser output are shown in Fig. 4. Table II gives the parameters for the instability threshold at various gas pressures.

The cw-laser threshold increases appreciably with increasing NH_3 pressure. This is plausible since in absence of pump radiation there is a sizable absorption on the FIR transition, which increases linearly with pressure and has to be overcome by the pumping.

It is noteworthy that the instability occurs for conditions where the laser transition is homogeneously broadened: The inhomogeneous ac-Stark broadening is appreciably smaller than the homogeneous linewidth.

Both the ac-Stark broadening and the homogeneous

broadening were determined by performing three-level calculations of the small signal gain employing the density matrix formalism, taking into account M degeneracy.⁷ We estimate that the "bad cavity" requirement is easily met under these conditions.

It has been found recently⁸ that, if the ratio of polarization and population decay rates $\gamma_{\parallel}/\gamma_{\perp} < \frac{1}{6}$, periodic solutions of the Lorenz equations do exist in the range of pump parameter values, where for $\gamma_{\parallel}/\gamma_{\perp} = 1$ chaos occurs.⁹ No precise values for population relaxation rates are known for this $^{15}\text{NH}_3$ transition. However, other NH_3 transition measurements report¹⁰ values around $\gamma_{\parallel}/\gamma_{\perp} = \frac{1}{6}$. Thus, a periodic lowest instability is not unexpected.

The ratios of instability-threshold pump intensity to cw laser-threshold pump intensity are, in effect, in the range which could be expected from the Lorenz model. It is not surprising that this quantity varies with pressure due to the equilibrium FIR absorption of the NH_3 . The low pressure value would therefore be better compared with calculations than the values at higher pressure.

In conclusion, for the homogeneously broadened ring laser we find a route to chaos with two counter-propagation modes as also reported for two-roll Bénard convection. In single-mode oscillation, an oscillatory instability is observed under conditions compatible with the Lorenz model.

ACKNOWLEDGMENTS

We would like to acknowledge helpful discussions with N. B. Abraham. This work was supported by the Deutsche Forschungsgemeinschaft.

¹It should be noted that the aim here is opposite to other work on FIR lasers, where the complex spectral structure of the gain line brought about by the ac-Stark effect (sometimes also referred to as "effect of Raman gain" or "effect of two-photon transitions"), is considered to further instabilities [N. M. Lawandy, *J. Opt. Soc. Am. B* **2**, 108 (1985)]. We intend to suppress the coherence in the interaction by shortening the phase memory of the molecules by means of collisions so that the gain line becomes homogeneously broadened.

²M. S. Feld and A. Javan, *Phys. Rev.* **177**, 540 (1969).

³H. Haken, *Phys. Lett.* **53A**, 77 (1975).

⁴H. Heppner and C. O. Weiss, *Appl. Phys. Lett.* **33**, 590 (1978).

⁵J. Maurer and A. Libchaber, *J. Phys. (Paris) Lett.* **40**, 419 (1979); A. Libchaber and J. Maurer, *J. Phys. (Paris) Colloq.* **41**, C3-51 (1980).

⁶G. L. Lippi, N. B. Abraham, F. T. Arecchi, N. Ridi, and J. R. Tredicce, *Opt. Commun.* (to be published).

⁷J. Heppner, C. O. Weiss, U. Hübner, and G. Schinn, *IEEE J. Quantum Electron.* **QE-16**, 392 (1980).

⁸L. M. Narducci, L. A. Lugiato, and N. B. Abraham (unpublished).

⁹H. Zeglache and P. Mandel, *J. Opt. Soc. Am. B* **2**, 18 (1985).

¹⁰T. Shimizu, F. O. Shimizu, R. Turner, and T. Oka, *J. Chem. Phys.* **55**, 2822 (1971); T. Shimizu, N. Morita, T. Kasuga, H. Sasada, F. Matsuhashima, and N. Konishi, *Appl. Phys.* **21**, 29 (1980).

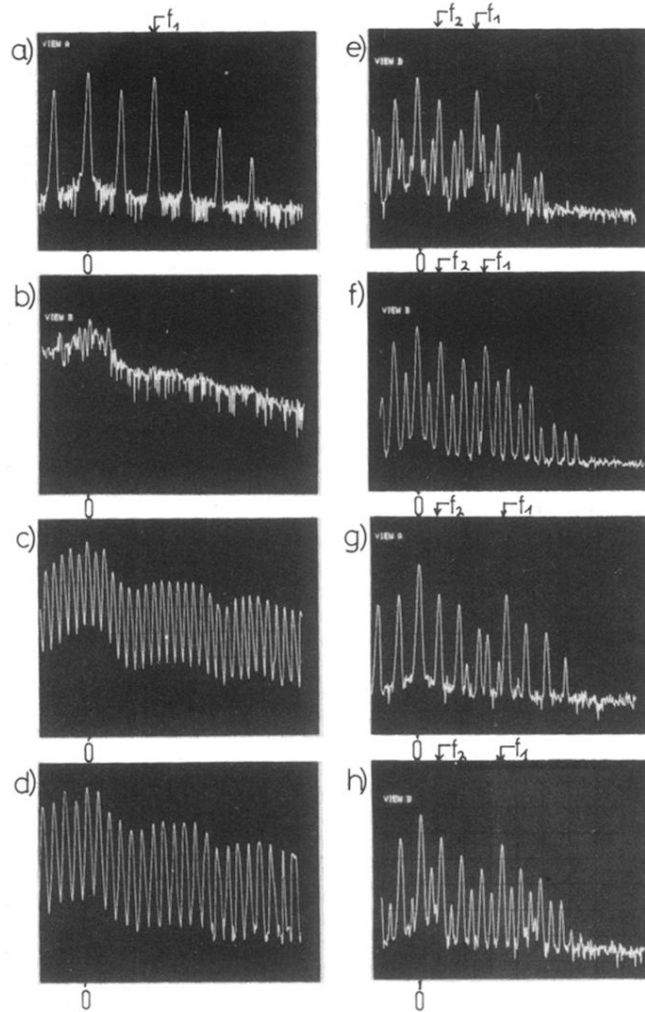


FIG. 2. Self-pulsing spectra of the two-mode ring laser. Vertical scale: 10 dB/division, horizontal scale: 500 kHz/division. (a) Period-doubled oscillation; (b) chaos; (c), (d) periodic windows above the threshold of chaotic emission; (e)–(h) two-frequency oscillation, phase locking, and period doubling; (e) f_2 slightly larger than $f_1/3$; (f) f_1 and f_2 lock at $f_2 = f_1/3$ and period double; (g) f_2 slightly smaller than $f_1/4$; (h) f_1 and f_2 lock at $f_2 = f_1/4$ and period double. Further period doublings following (f) and (h) lead to chaos. Also, phase locking at higher harmonics of f_2 was observed. Period doubling cascade between (a) and (b) as well as fundamental frequency preceding (a) left out for brevity. It was undecidable in the experiment whether (a) corresponds to a single-frequency oscillation or to an $f_2 = f_1/2$ locked state.

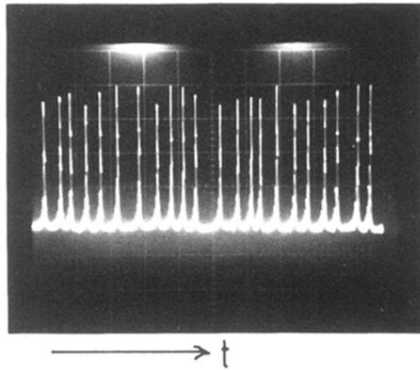


FIG. 3. Time picture of chaotic emission of two-mode NH₃ ring laser corresponding to the spectrum given in [Fig. 2(b)]: horizontal scale 50 μ s/division.

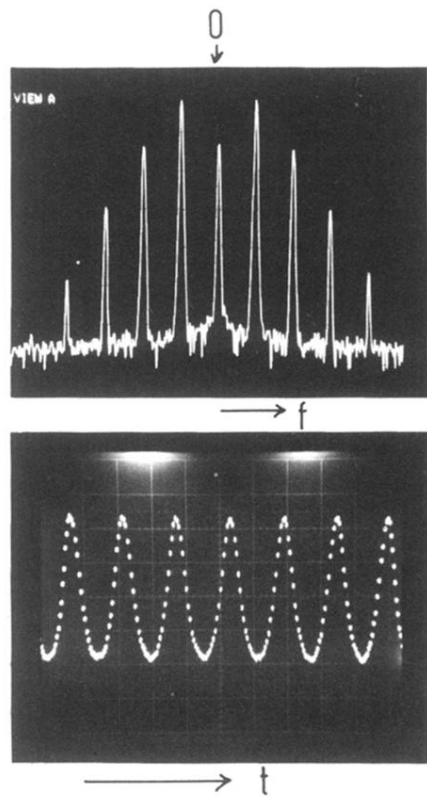


FIG. 4. Single-mode NH_3 ring-laser instability. NH_3 pressure 7 Pa, pump intensity 1 W/cm^2 . (a) rf spectrum, horizontal scale 1 MHz/division. (b) Time picture, horizontal scale $1 \mu\text{s/division}$.